Available online at www.sciencedirect.com
ScienceDirect
Information Fusion 9 (2008) 450–464
INFORMATION FUSION
www.elsevier.com/locate/inffus

The coordination generalized particle model—An evolutionary approach to multi-sensor fusion

Xiang Feng [a,*], Francis C.M. Lau [a], Dianxun Shuai [b]

[a] Department of Computer Science, The University of Hong Kong, Hong Kong
[b] Department of Computer Science and Engineering, East China University of Science and Technology, Shanghai 200237, PR China

Received 9 November 2006; received in revised form 6 January 2007; accepted 6 January 2007
Available online 14 January 2007

Abstract

The rising popularity of multi-source, multi-sensor networks supporting real-life applications calls for an efficient and intelligent approach to information fusion. Traditional optimization techniques often fail to meet the demands. The evolutionary approach provides a valuable alternative due to its inherent parallel nature and its ability to deal with difficult problems. We present a new evolutionary approach based on the *coordination generalized particle model* (C-GPM) which is founded on the laws of physics. C-GPM treats sensors in the network as distributed intelligent agents with various degrees of autonomy. Existing approaches based on intelligent agents cannot completely answer the question of how their agents could coordinate their decisions in a complex environment. The proposed C-GPM approach can model the autonomy of as well as the social coordinations and interactive behaviors among sensors in a decentralized paradigm. Although the other existing evolutionary algorithms have their respective advantages, they may not be able to capture the entire dynamics inherent in the problem, especially those that are high-dimensional, highly nonlinear, and random. The C-GPM approach can overcome such limitations. We develop the C-GPM approach as a physics-based evolutionary approach that can describe such complex behaviors and dynamics of multiple sensors.

Keywords: Multi-sensor fusion; Sensor behavior; Sensor coordination; Evolutionary algorithm; Dynamic sensor resource allocation problem; Coordination generalized particle model (C-GPM)

1. Introduction

Sensor fusion is a method of integrating signals from multiple sources into a single signal or piece of information. These sources are sensors or devices that allow for perception or measurement of the changing environment. The method uses ''sensor fusion'' or ''data fusion'' algorithms which can be classified into different groups, including (1) fusion based on probabilistic models, (2) fusion based on least-squares techniques, and (3) intelligent fusion. This paper presents an evolutionary approach to intelligent information fusion.

Many applications in multi-sensor information fusion can be stated as optimization problems. Among the many different optimization techniques, evolutionary algorithms (EA) are a heuristic-based global search and optimization methods that have found their way into almost every area of real world optimization problems. EA provide a valuable alternative to traditional methods because of their inherent parallelism and their ability to deal with difficult problems that feature non-homogeneous, noisy, incomplete and/or obscured information, constrained resources, and massive processing of large amounts of data. Traditional methods based on correlation, mutual information, local optimization, and sequential processing may perform poorly. EA are inspired by the principles of natural evolution and genetics. Popular EA include genetic algorithm (GA) [1], simulated annealing algorithm (SA) [2], ant

* Corresponding author. Tel.: +852 28578442; fax: +852 25598447.
E-mail address: xfeng@cs.hku.hk (X. Feng).

1566-2535/$ - see front matter © 2007 Elsevier B.V. All rights reserved.
doi:10.1016/j.inffus.2007.01.001

colony optimization (ACO) [3], particle swarm optimization (PSO) [4], etc., which have all been featured in either Nature or Science.

In this paper, we propose the C-GPM approach as a new branch of EA, which is based on the laws of physics. Just like other EA drawing from observations of physical processes that occur in nature, the C-GPM approach is inspired by physical models of particle dynamics. Although the other existing EA have their respective advantages, they may not be able to capture the entire dynamics inherent in the problem, especially those that are high-dimensional, highly nonlinear, and random. The C-GPM approach can overcome such limitations. We develop the C-GPM approach as a physics-based evolutionary approach that can describe the complex behaviors and dynamics arising from interactions among multiple sensors.

Our C-GPM algorithm, just like the other popular EA mentioned above, belongs to the class of meta-heuristics in artificial intelligence, which are approximate algorithms for obtaining good enough solutions to hard combinatorial optimization problems in a reasonable amount of computation time.

Similar to the other EA, the C-GPM algorithm is inherently parallel and can perform well in providing approximating solutions to all types of problems. EA applied to the modeling of biological evolution are generally limited to explorations of micro-evolutionary processes. Some computer simulations, such as Tierra and Avida, however, attempt to model macro-evolutionary dynamics. C-GPM algorithm is an exploration of micro-evolutionary processes.

In the physical world, mutual attraction between particles causes motion. The reaction of a particle to the field of potential would change the particle's coordinates and energies. The change in the state of the particle is a result of the influence of the potential. In C-GPM, each particle is described by some differential dynamic equations, and the results of their calculations govern the movement (to a new state in the field) of the particle. Specifically, each particle computes the combined effect of its own autonomous self-driving force, the field potential and the interaction potential. If the particles cannot eventually reach an equilibrium, they will proceed to execute a goal-satisfaction process.

In summary, the relative differences between our C-GPM algorithm and other popular EA can be seen in Table 1. The common features of these different approaches are listed as follows:

- They draw from observations of physical processes that occur in nature.
- They belong to the class of meta-heuristics, which are approximate algorithms used to obtain good enough solutions to hard combinatorial optimization problems in a reasonable amount of computation time.
- They have inherent parallelism and the ability to deal with difficult problems.
- They consistently perform well in finding approximating solutions to all types of problems.
- They are mainly used in the fields of artificial intelligence.

In this paper, we study some theoretical foundations of the C-GPM approach including the convergence of C-GPM. The structure of the paper is as follows. In Section 2, we discuss and formalize the problem model for the typical multi-sensor system. In Section 3, we present the evolutionary C-GPM approach to intelligent multi-sensor information fusion. In Section 4, we describe an experiment to verify the claimed properties of the approach. We draw conclusion in Section 5.

2. Dynamic sensor resource allocation

In a sensor-based application with command and control, a major prerequisite to the success of the command and control process is the effective use of the scarce and costly sensing resources. These resources represent an important source of information on which the command and control process bases most of its reasoning. Whenever there are insufficient resources to perform all the desired tasks, the sensor management must allocate the available sensors to those tasks that could maximize the effectiveness of the sensing process.

Table 1
The C-GPM algorithm vs. other popular EA

	C-GPM	GA	SA	ACO	PSO
Inspired by	Physical models of particle dynamics	Natural evolution	Thermodynamics	Behaviors of real ants	Biological swarm (e.g., swarm of bees)
Key components	Energy function; differential dynamic equations	Chromosomes	Energy function	Pheromone laid	Velocity-coordinate model
Exploration	Both macro-evolutionary and micro-evolutionary processes	Macro-evolutionary processes	Micro-evolutionary processes	Macro-evolutionary processes	Macro-evolutionary
Dynamics	Can capture the entire dynamics inherent in the problem	Cannot capture	Can capture partly	Cannot capture	Cannot capture
High-dimensional, highly nonlinear, random behaviors and dynamics	Can describe	Cannot describe	Can describe partly	Cannot describe	Cannot describe

Table 2
The matrix $\mathscr{S}(t)$

Sensors	Objects				
	T_1	...	T_k	...	T_m
A_1	$r_{11}, c_{11}, x_{11}, \zeta_{11}$	...	$r_{1k}, c_{1k}, x_{1k}, \zeta_{1k}$	...	$r_{1m}, c_{1m}, x_{1m}, \zeta_{1m}$
A_i	$r_{i1}, c_{i1}, x_{i1}, \zeta_{i1}$	...	$r_{ik}, c_{ik}, x_{ik}, \zeta_{ik}$	...	$r_{im}, c_{im}, x_{im}, \zeta_{im}$
A_n	$r_{n1}, c_{n1}, x_{n1}, \zeta_{n1}$	...	$r_{nk}, c_{nk}, x_{nk}, \zeta_{nk}$	...	$r_{nm}, c_{nm}, x_{nm}, \zeta_{nm}$

The dynamic sensor allocation problem consists of selecting sensors of a multi-sensor system to be applied to various objects of interest using feedback strategies. Consider the problem of n sensors, $\mathscr{A} = \{A_1, \ldots, A_n\}$, and m objects, $\mathscr{T} = \{T_1, \ldots, T_m\}$. In order to obtain useful information about the state of each object, appropriate sensors should be assigned to various objects at the time intervals $t \in \{0, 1, \ldots, T-1\}$. The collection of sensors applied to object k during interval t is represented by a vector $X_k(t) = \{x_{1k}, \ldots, x_{ik}, \ldots, x_{nk}\}$, where

$$x_{ik}(t) = \begin{cases} 1 & \text{if sensor } i \text{ is used on object } k \text{ at interval } t \\ 0 & \text{otherwise} \end{cases}$$

Because of the limited resources sustaining the whole system, the planned sensor distributions must satisfy the following constraint for every $t \in \{0, 1, \ldots, T-1\}$:

$$\sum_{k=1}^{m} r_{ik}(t) x_{ik}(t) = 1 \tag{1}$$

where r_{ik} denotes that quantity of resources consumed by sensor i on object k and $0 \leqslant r_{ik} \leqslant 1$.

The goal of sensor allocation is to try to achieve an optimal allocation of all sensors to all the objects after T stages. Let $C = (c_{ik})_{n\times m}$ be a two-dimensional weight vector. Sensor allocation can be defined as a problem to find a two-dimensional allocation vector $R = (r_{ik})_{n\times m}$, which maximizes the objective in (2), subject to the constraint (1)

$$z(R) = (C)^{\mathrm{T}} R X = \sum_{i=1}^{n} \sum_{k=1}^{m} c_{ik} r_{ik} x_{ik} \tag{2}$$

Let $\zeta_{ik}(t)$ represent the intention strength of social coordination. Thus we obtain an allocation-related matrix $\mathscr{S}(t) = [s_{ik}(t)]_{n\times m}$, as shown in Table 2, where $s_{ik}(t) = \langle r_{ik}(t), c_{ik}(t), x_{ik}(t), \zeta_{ik}(t)\rangle$. For convenience, both $r_{ik}(t)$ and $c_{ik}(t)$ are normalized such that $0 \leqslant r_{ik}(t) \leqslant 1$ and $0 \leqslant c_{ik}(t) \leqslant 1$.

3. The C-GPM approach to sensor fusion

3.1. Physical model of C-GPM

This subsection discusses the physical meanings of the *coordination generalized particle model* (C-GPM) for sensor fusion in multi-sensor systems which involve social coordinations among the sensors. C-GPM treats every entry of the allocation-related matrix $\mathscr{S}_{ik}$ as a particle, s_{ik}, in a force field. The problem solving process is hence transformed into one dealing with the kinematics and dynamics of particles in the force field. The s_{ik}'s form the matrix $\mathscr{S}_{ik}$. For convenience, we let s_{ik} represent both an entry of the matrix as well as its corresponding particle in the force field.

Particle and *force-field* are two concepts of physics. Particles in our C-GPM move not only under outside forces, but also under internal force; hence in this sense, they are somewhat different from particles in physics.

As shown in Fig. 1, the vertical coordinate of a particle s_{ik} in force field F represents the utility obtained by sensor $\mathscr{A}_i$ from being used on object $\mathscr{T}_k$. A particle experiences several kinds of forces simultaneously, which include the gravitational force of the force field, the pulling or pushing forces due to social coordinations among the sensors, and the particle's own autonomous driving force. The forces on a particle are handled only along the vertical direction. Thus a particle will be driven by the resultant force of all the forces that act on it upwards or downwards along the vertical direction. The larger the upward/downward resultant force on a particle, the faster the upward/downward motion of the particle. When the resultant force on a particle is equal to zero, the particle will stop moving, being in an equilibrium state.

The upward gravitational force of the force field contributes an upward component of a particle's motion, which represents the tendency that the particle pursues the collective benefit of the whole multi-sensor system. The other upward or downward components of the particle's motion, which are related to the social coordinations among the sensors, depend on the strengths and kinds of these coordinations. The pulling or pushing forces among particles make particles move to satisfy resource restrictions, as well as reflect the social coordinations and behaviors among the sensors. A particle's own autonomous driving force is directly proportional to the degree the particle tries to maximize its own profit (utility). This autonomous driving force of a particle actually sets the C-GPM approach apart from the classical physical model. All the generalized particles simultaneously move in the force field, and once they have all reached their respective equilibrium positions, we have a feasible solution to the optimization problem in question.

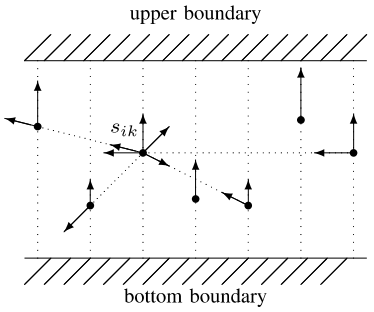

Fig. 1. The force field and the particles.

Because the problem in this paper is a one objective problem, we limit the particles movements to one dimension. The design of C-GPM in fact allows forces of all directions to exist. These forces can be decomposed into their horizontal and vertical components. In this present work, only the vertical component may affect a particle's motion. In a forthcoming paper, we will introduce the multiple objectives problem where we will handle particles' movements along multiple dimensions.

3.2. Mathematical model of C-GPM

We define in this subsection the mathematical model of C-GPM for the sensor allocation problem that involves n sensors and m objects.

Let $u_{ik}(t)$ be the distance from the current position of particle s_{ik} to the bottom boundary of force field F at time t, and let $J(t)$ be the utility sum of all particles, which we define as follows:

$$\begin{aligned} u_{ik}(t) &= \mathrm{a}[1-\exp(-c_{ik}(t)r_{ik}(t)x_{ik}(t))] \\ J(t) &= \sum_{i=1}^{n}\sum_{k=1}^{m} u_{ik}(t) \end{aligned} \tag{3}$$

where $0 < \mathrm{a} < 1$. $1-\mathrm{e}^{-x}$ is chosen as the definition of u_{ik} because $1-\mathrm{e}^{-x}$ is a monotone increasing function and between 0 and 1 (Fig. 2).

At time t, the potential energy functions, $P(t)$, which is caused by the upward gravitational force of force field F, is defined by

$$P(t) = \epsilon^2 \ln \sum_{i=1}^{n}\sum_{k=1}^{m} \exp[-u_{ik}^2(t)/2\epsilon^2] - \epsilon^2 \ln mn \tag{4}$$

where $0 < \epsilon < 1$. The smaller $P(t)$ is, the better. With Eq. (4), we attempt to construct a potential energy function, $P(t)$, such that the decrease of its value would imply the increase of the minimal utility of all the sensors. We prove it in Proposition 3. This way we can optimize the multi-sensor fusion problem in the sense that we consider not only the aggregate utility, but also the individual personal utilities, especially the minimum one. In addition, ϵ represents the strength of upward gravitational force of the force field. The bigger ϵ is, the better. If we did not get a sufficiently satisfactory result by C-GPM, we can let ϵ smaller.

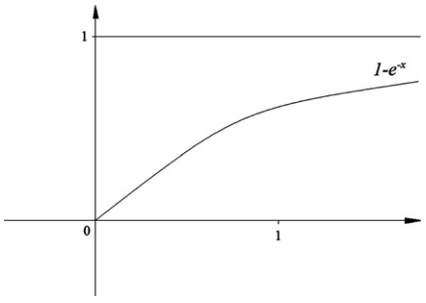

Fig. 2. Graphical presentation of $u_{ik}(t)$.

Table 3
Social coordinations among sensors

β_{ijk}	Type	Name	ζ_{ijk}
I	A_{ijk}	Adaptive avoidance coordination	−1
	B_{ijk}	Adaptive exploitation coordination	
	C_{ijk}	Collaboration coordination	
II	D_{ijk}	Tempting avoidance coordination	1
	E_{ijk}	Tempting exploitation coordination	
	F_{ijk}	Deception coordination	
III	G_{ijk}	Competition coordination	1
	H_{ijk}	Coalition coordination	
	I_{ijk}	Habituation/preference coordination	
IV	J_{ijk}	Antagonism coordination	−1
	K_{ijk}	Reciprocation coordination	
	L_{ijk}	Compromise coordination	

The gravitational force of the force field causes the particles to move to increase the corresponding sensors' minimal personal utility, and hence to realize max–min fair allocation and increase the whole utility of the multi-sensor system.

Following the literature [5–8], we divide typical social coordinations between sensor A_i and sensor A_j into 12 possible types, as in Table 3.

A_{ijk}: To avoid the harmful consequence possibly caused by A_j, A_i wants to change its own current intention. B_{ijk}: To exploit the beneficial consequence possibly caused by A_j, A_i wants to change its own current intention. C_{ijk}: To benefit A_j, A_i wants to change its own current intention regardless of self-benefit. D_{ijk}: A_i tries to allure A_j to modify A_j's current intention so that A_i could avoid the harmful consequence possibly caused by A_j. E_{ijk}: A_i tries to entice A_j to modify A_j's current intention so that A_i could exploit the beneficial consequence possibly caused by A_j. F_{ijk}: A_i tries to tempt A_j to modify A_j's current intention so that A_i might benefit from this, while A_j's interests might be infringed. G_{ijk}: To compete with each other, neither A_i nor A_j will modify their own intention, but both A_i and A_j might enhance their intention strengths with respect to the Kth goal (or object). H_{ijk}: Neither A_i nor A_j will modify their own current intention, but both A_i and A_j might decrease their intention strengths with respect to the Kth goal. I_{ijk}: Due to disregard of the other side, neither A_i nor A_j will modify their own current intention. J_{ijk}: To harm the other side, both A_i and A_j try to modify their own current intentions. K_{ijk}: Both A_i and A_j try to modify their own current intentions so that they could implement the intention of the other side. L_{ijk}: Both A_i and A_j try to modify their current intentions so that they can do something else.

Of the 12 types of social coordination, types A, B, C, D, E and F and F are via unilateral communication, and types G, H, I, J, K and L by bilateral communication. Based on which sensor(s) will modify their current intention, the 12 types can be conveniently grouped into the four categories. For A_{ijk}, B_{ijk}, C_{ijk}, it is A_i; for D_{ijk}, E_{ijk}, F_{ijk}, it is A_j; for

G_{ijk}, H_{ijk}, I_{ijk}, none will; and for J_{ijk}, K_{ijk}, L_{ijk}, both A_i and A_j will, and so we have

$$\mathscr{L}^{(\mathrm{I})} = \mathscr{L}^{(10)} = \{A_{ijk}, B_{ijk}, C_{ijk} | \forall i,j,k\},$$
$$\mathscr{L}^{(\mathrm{II})} = \mathscr{L}^{(01)} = \{D_{ijk}, E_{ijk}, F_{ijk} | \forall i,j,k\},$$
$$\mathscr{L}^{(\mathrm{III})} = \mathscr{L}^{(00)} = \{G_{ijk}, H_{ijk}, I_{ijk} | \forall i,j,k\},$$
$$\mathscr{L}^{(\mathrm{IV})} = \mathscr{L}^{(11)} = \{J_{ijk}, K_{ijk}, L_{ijk} | \forall i,j,k\},$$
$$\mathscr{L} = (\mathscr{L}^{(01)} \cup \mathscr{L}^{(10)} \cup \mathscr{L}^{(10)} \cup \mathscr{L}^{(11)}).$$

The intention strength $\zeta_{ik}(t)$ of sensor A_i with respect to object T_k is defined by

$$\zeta_{ik}(t) = \sum_{j=1}^{n} \zeta_{ijk}(t) + \sum_{j=1}^{n} \zeta_{jik}(t) \tag{5}$$

$$\zeta_{ijk}(t) = \begin{cases} 1 & \text{if } \beta_{ijk} \in \mathscr{L}^{(\mathrm{II})} \cup \mathscr{L}^{(\mathrm{III})} \\ -1 & \text{if } \beta_{ijk} \in \mathscr{L}^{(\mathrm{I})} \cup \mathscr{L}^{(\mathrm{IV})} \end{cases}$$
$$\zeta_{jik}(t) = \begin{cases} 1 & \text{if } \beta_{jik} \in \mathscr{L}^{(\mathrm{I})} \cup \mathscr{L}^{(\mathrm{III})} \\ -1 & \text{if } \beta_{jik} \in \mathscr{L}^{(\mathrm{II})} \cup \mathscr{L}^{(\mathrm{IV})} \end{cases} \tag{6}$$

β_{ijk} is the social coordination of sensor A_i with respect to sensor A_j for object T_k, which gives rise to the change $\zeta_{ijk}(t)$ of intention strength $\zeta_{ik}(t)$.

$\zeta_{ik}(t)$ of $s_{ik}(t)$ represents the aggregate intention strength when more than one social coordination happen simultaneously at time t. The greater $\zeta_{ik}(t)$ is, the more necessary would sensor A_i have to modify its $r_{ik}(t)$ for object T_k.

At time t, the potential energy function, $Q(t)$, is defined by

$$Q(t) = \sum_{i=1}^{n} \left| \sum_{k=1}^{m} r_{ik}(t) x_{ik}(t) - 1 \right|^2 - \sum_{i,k} \int_0^{u_{ik}} \{[1 + \exp(-\zeta_{ik} x)]^{-1} - 0.5\} \, \mathrm{d}x \tag{7}$$

The first term of $Q(t)$ is related to the constraints on the sensors' capability; the second term involves social coordinations among the sensors, with ζ_{ik} coming from Eqs. (5) and (6). The first term of $Q(t)$ corresponds to a penalty function with respect to the constraint on the utilization of resources. Therefore, the sensors' resource utilization can be explicitly included as optimization objectives in the multi-sensor fusion problem. The second term of $Q(t)$ is chosen as shown because we want $\frac{\partial Q}{\partial u_{ik}}$ to be a monotone decreasing sigmoid function, as shown in Fig. 3. $-\{[1 + \exp(-\zeta_{ik} u_{ik})]^{-1} - 0.5\}$ is such a function. Therefore we let $\frac{\partial Q}{\partial u_{ik}}$ equal to $-\{[1 + \exp(-\zeta_{ik} u_{ik})]^{-1} - 0.5\}$. Then $\frac{\partial Q}{\partial u_{ik}}$ is integrated to be Q.

A particle in the force field can move upward along a vertical line under a composite force making up of

- the upward gravitational force of the force field,
- the upward or downward component of particle motion that is related to social coordinations among the sensors,
- the pulling or pushing forces among the particles in order to satisfy resource restrictions, and
- the particle's own autonomous driving force.

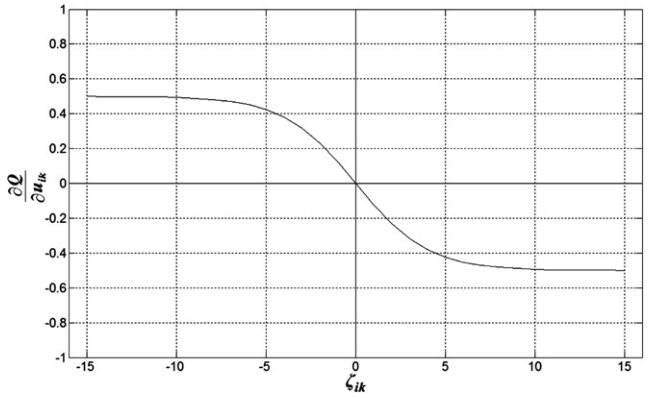

Fig. 3. Graphical presentation of $\frac{\partial Q}{\partial u_{ik}}$.

The four kinds of forces can all contribute to the particles' upward movements. What is more, these forces produce hybrid potential energy of the force field. The general hybrid potential energy function for particle s_{ik}, $E_{ik}(t)$, can be defined by

$$E_{ik}(t) = \lambda_1 u_{ik}(t) + \lambda_2 J(t) - \lambda_3 P(t) - \lambda_4 Q(t) \tag{8}$$

where $0 < \lambda_1, \lambda_2, \lambda_3, \lambda_4 < 1$.

Dynamic equations for particle s_{ik} is defined by

$$\begin{cases} \mathrm{d}u_{ik}(t)/\mathrm{d}t = \Psi_1(t) + \Psi_2(t) \\ \Psi_1(t) = -u_{ik}(t) + \gamma v_{ik}(t) \\ \Psi_2(t) = \left[\lambda_1 + \lambda_2 \frac{\partial J(t)}{\partial u_{ik}(t)} - \lambda_3 \frac{\partial P(t)}{\partial u_{ik}(t)} - \lambda_4 \frac{\partial Q(t)}{\partial u_{ik}(t)}\right] \\ \qquad \left\{ \left[\frac{\partial u_{ik}(t)}{\partial r_{ik}(t)}\right]^2 + \left[\frac{\partial u_{ik}(t)}{\partial c_{ik}(t)}\right]^2 \right\} \end{cases} \tag{9}$$

where $\gamma > 1$. And $v_{ik}(t)$ is a piecewise linear function of $u_{ik}(t)$ defined by

$$v_{ik}(t) = \begin{cases} 0 & \text{if } u_{ik}(t) < 0 \\ u_{ik}(t) & \text{if } 0 \leqslant u_{ik}(t) \leqslant 1 \\ 1 & \text{if } u_{ik}(t) > 1 \end{cases} \tag{10}$$

In order to dynamically optimize sensor allocation, the particle s_{ik} may alternately modify r_{ik} and c_{ik}, respectively, as follows:

$$\mathrm{d}c_{ik}(t)/\mathrm{d}t = \lambda_1 \frac{\partial u_{ik}(t)}{\partial c_{ik}(t)} + \lambda_2 \frac{\partial J(t)}{\partial c_{ik}(t)} - \lambda_3 \frac{\partial P(t)}{\partial c_{ik}(t)} - \lambda_4 \frac{\partial Q(t)}{\partial c_{ik}(t)} \tag{11}$$

$$\mathrm{d}r_{ik}(t)/\mathrm{d}t = \lambda_1 \frac{\partial u_{ik}(t)}{\partial r_{ik}(t)} + \lambda_2 \frac{\partial J(t)}{\partial r_{ik}(t)} - \lambda_3 \frac{\partial P(t)}{\partial r_{ik}(t)} - \lambda_4 \frac{\partial Q(t)}{\partial r_{ik}(t)} \tag{12}$$

where $\frac{\partial Q(t)}{\partial u_{ik}(t)} = -\{[1 + \exp(-\zeta_{ik}(t) u_{ik}(t))]^{-1} - 0.5\}$ is a sigmoid function of the aggregate intention strength $\zeta_{ik}(t)$. The graphical presentation of $\frac{\partial Q}{\partial u_{ik}}$ is shown in Fig. 3.

Note that $\zeta_{ik}(t)$ is related to social coordinations among the sensors at time t. $\frac{\partial Q}{\partial u_{ik}}$ is a monotone decreasing function. By Eq. (9) the greater the value of $\zeta_{ik}(t)$, the more there are

values of $\Psi_2(t)$ and hence $u_{ik}(t)$ will increase, which implies that the social coordinations will strengthen the current allocation $r_{ik}(t)$.

Because $\frac{\partial Q}{\partial u_{ik}}$ is a monotone decreasing function, the greater the value of $\zeta_{ik}(t)$, the smaller $\frac{\partial Q}{\partial u_{ik}}$, the greater $-\frac{\partial Q}{\partial u_{ik}}$, the greater $\Psi_2(t)$ by Eq. (9) and the greater $\Delta r_{ik}(t+1)$ by Eq. (12). Since $r_{ik}(t+1) = r_{ik}(t) + \Delta r_{ik}(t+1)$, the greater the value of $\zeta_{ik}(t)$, the greater $r_{ik}(t+1)$. Since u_{ik} is a monotone increasing function, the greater $r_{ik}(t+1)$, the greater u_{ik}

$$\zeta_{ik}(t)\uparrow \Rightarrow \frac{\partial Q}{\partial u_{ik}}\downarrow \Rightarrow -\frac{\partial Q}{\partial u_{ik}}\uparrow \overset{(9)}{\Rightarrow} \Psi_2\uparrow -\frac{\partial Q}{\partial u_{ik}}\uparrow \overset{(11)}{\Rightarrow} \Delta r_{ik}(t+1)\uparrow \overset{a}{\Rightarrow} r_{ik}(t+1)\uparrow \underset{b}{\overset{(3)}{\Rightarrow}} u_{ik}\uparrow$$

(a) $r_{ik}(t+1) = r_{ik}(t) + \Delta r_{ik}(t+1)$;
(b) u_{ik} is monotone increasing function.

In the following, we derive some formal properties of the mathematical model presented above.

Proposition 1. *Updating the weights c_{ik} and allotted resource r_{ik} by Eqs. (11) and (12) respectively amounts to changing the speed of particle s_{ik} by $\Psi_2(t)$ of Eq. (9).*

Denote the jth terms of Eqs. (11) and (12) by $\left\langle \frac{\mathrm{d}c_{ik}(t)}{\mathrm{d}t}\right\rangle_j$ and $\left\langle \frac{\mathrm{d}r_{ik}(t)}{\mathrm{d}t}\right\rangle_j$, respectively. When allotted resource r_{ik} is updated according to (12), the first and second terms of (12) will cause the following speed increments of the particle s_{ik}, respectively:

$$\langle \mathrm{d}u_{ik}(t)/\mathrm{d}t\rangle_1^r = \frac{\partial u_{ik}(t)}{\partial r_{ik}(t)}\left\langle \frac{\mathrm{d}r_{ik}(t)}{\mathrm{d}t}\right\rangle_1 = \lambda_1\left[\frac{\partial u_{ik}(t)}{\partial r_{ik}(t)}\right]^2 \tag{13}$$

$$\begin{aligned}\langle \mathrm{d}u_{ik}(t)/\mathrm{d}t\rangle_2^r &= \frac{\partial u_{ik}(t)}{\partial r_{ik}(t)}\left\langle \frac{\mathrm{d}r_{ik}(t)}{\mathrm{d}t}\right\rangle_2 = \lambda_2\frac{\partial u_{ik}(t)}{\partial r_{ik}(t)}\frac{\partial J(t)}{\partial r_{ik}(t)}\\ &= \lambda_2\frac{\partial u_{ik}(t)}{\partial r_{ik}(t)}\frac{\partial J(t)}{\partial u_{ik}(t)}\frac{\partial u_{ik}(t)}{\partial r_{ik}(t)}\\ &= \lambda_2\frac{\partial J(t)}{\partial u_{ik}(t)}\left[\frac{\partial u_{ik}(t)}{\partial r_{ik}(t)}\right]^2\end{aligned} \tag{14}$$

Similarly, the third and the fourth term of Eq. (12) will cause the following speed increments of the particle s_{ik}:

$$\begin{aligned}\langle \mathrm{d}u_{ik}(t)/\mathrm{d}t\rangle_3^r &= -\lambda_3\frac{\partial P(t)}{\partial u_{ik}(t)}\left[\frac{\partial u_{ik}(t)}{\partial r_{ik}(t)}\right]^2\langle \mathrm{d}u_{ik}(t)/\mathrm{d}t\rangle_4^r\\ &= -\lambda_4\frac{\partial Q(t)}{\partial u_{ik}(t)}\left[\frac{\partial u_{ik}(t)}{\partial r_{ik}(t)}\right]^2\end{aligned}$$

Similarly, for Eq. (11), we have $\langle \mathrm{d}u_{ik}(t)/\mathrm{d}t\rangle_j^c,\ j = 1,2,3,4$. We thus obtain

$$\begin{aligned}&\sum_{j=1}^{4}[\langle \mathrm{d}u_{ik}(t)/\mathrm{d}t\rangle_j^c + \langle \mathrm{d}u_{ik}(t)/\mathrm{d}t\rangle_j^r]\\ &= \left[\lambda_1 + \lambda_2\frac{\partial J(t)}{\partial u_{ik}(t)} - \lambda_3\frac{\partial P(t)}{\partial u_{ik}(t)} - \lambda_4\frac{\partial Q(t)}{\partial u_{ik}(t)}\right]\left\{\left[\frac{\partial u_{ik}(t)}{\partial r_{ik}(t)}\right]^2 + \left[\frac{\partial u_{ik}(t)}{\partial c_{ik}(t)}\right]^2\right\} = \Psi_2(t).\end{aligned}$$

Therefore, updating $c_{ik}^{(j)}$ and $r_{ik}^{(j)}$ by (11) and (12), respectively, gives rise to the speed increment of particle s_{ik} that is exactly equal to $\Psi_2(t)$ of Eq. (9).

Proposition 2. *The first and second terms of Eqs. (11) and (12) will enable the particle s_{ik} to move upwards, that is, the personal utility of sensor A_i from object T_k increases, in direct proportion to the value of $(\lambda_1 + \lambda_2)$.*

According to Eqs. (13) and (14), the sum of the first and second terms of Eqs. (11) and (12) will be

$$\begin{aligned}&\langle \mathrm{d}u_{ik}(t)/\mathrm{d}t\rangle_1^r + \langle \mathrm{d}u_{ik}(t)/\mathrm{d}t\rangle_2^r + \langle \mathrm{d}u_{ik}(t)/\mathrm{d}t\rangle_1^c + \langle \mathrm{d}u_{ik}(t)/\mathrm{d}t\rangle_2^c\\ &= \left[\lambda_1 + \lambda_2\frac{\partial J(t)}{\partial u_{ik}(t)}\right]\left\{\left[\frac{\partial u_{ik}(t)}{\partial r_{ik}(t)}\right]^2 + \left[\frac{\partial u_{ik}(t)}{\partial c_{ik}(t)}\right]^2\right\}\\ &= (\lambda_1 + \lambda_2)x_{ik}^2(t)[r_{ik}^2(t) + c_{ik}^2(t)][-u_{ik}(t)]^2 \geqslant 0.\end{aligned}$$

Therefore, the first and second terms of (11) and (12) will cause $u_{ik}(t)$ to monotonically increase.

Proposition 3. *For C-GPM, if ϵ is very small, then decreasing the potential energy $P(t)$ of Eq. (4) amounts to increasing the minimal utility of an sensor with respect to an object, minimized over $\mathscr{S}(t)$.*

Supposing that $H(t) = \max_{i,k}\{-u_{ik}^2(t)\}$, we have

$$\begin{aligned}[\exp(H(t)/2\epsilon^2)]^{2\epsilon^2} &\leqslant \left[\sum_{i=1}^{n}\sum_{k=1}^{m}\exp(-u_{ik}^2(t)/2\epsilon^2)\right]^{2\epsilon^2}\\ &\leqslant [mn\exp(H(t)/2\epsilon^2)]^{2\epsilon^2}.\end{aligned}$$

Taking the logarithm of both sides of the above inequalities gives

$$H(t) \leqslant 2\epsilon^2\ln\sum_{i=1}^{n}\sum_{k=1}^{m}\exp(-u_{ik}^2(t)/2\epsilon^2) \leqslant H(t) + 2\epsilon^2\ln mn.$$

Since mn is constant and ϵ is very small, we have

$$H(t) \approx 2\epsilon^2\ln\sum_{i=1}^{n}\sum_{k=1}^{m}\exp(-u_{ik}^2(t)/2\epsilon^2) - 2\epsilon^2\ln mn = 2P(t).$$

It turns out that the potential energy $P(t)$ at the time t represents the maximum of $-u_{ik}^2(t)$ among all the particles s_{ik}, which is the minimal personal utility of a sensor with respect to an object at time t. Hence the decrease of potential energy $P(t)$ will result in the increase of the minimum of $u_{ik}(t)$.

Proposition 4. *Updating c_{ik} and r_{ik} according to Eqs. (11) and (12) amounts to increasing the minimal utility of a sensor with respect to an object in direct proportion to the value of λ_3.*

The speed increment of particle s_{ik}, which is related to potential energy $P(t)$, is given by

$$\begin{aligned}\left\langle \frac{\mathrm{d}u_{ik}(t)}{\mathrm{d}t}\right\rangle_3 &= \langle \mathrm{d}u_{ik}(t)/\mathrm{d}t\rangle_3^r + \langle \mathrm{d}u_{ik}(t)/\mathrm{d}t\rangle_3^c\\ &= -\lambda_3\frac{\partial P(t)}{\partial u_{ik}(t)}\left\{\left[\frac{\partial u_{ik}(t)}{\partial r_{ik}(t)}\right]^2 + \left[\frac{\partial u_{ik}(t)}{\partial c_{ik}(t)}\right]^2\right\}.\end{aligned}$$

Denote by $\left\langle \frac{dP(t)}{dt} \right\rangle$ the differentiation of the potential energy function $P(t)$ with respect to time t arising from using (11) and (12). We have

$$\begin{aligned}\left\langle \frac{dP(t)}{dt} \right\rangle &= \frac{\partial P(t)}{\partial u_{ik}(t)} \left\langle \frac{du_{ik}(t)}{dt} \right\rangle_3 \\ &= -\lambda_3 \left[\frac{\partial P(t)}{\partial u_{ik}(t)}\right]^2 \left\{ \left[\frac{\partial u_{ik}(t)}{\partial r_{ik}(t)}\right]^2 + \left[\frac{\partial u_{ik}(t)}{\partial c_{ik}(t)}\right]^2 \right\} \\ &= -\lambda_3 \omega_{ik}^2(t) u_{ik}^2(t) x_{ik}^2(t) [r_{ik}^2(t) + c_{ik}^2(t)][u_{ik}(t)]^2 \leqslant 0.\end{aligned}$$

where,

$$\omega_{ik}(t) = \exp[-u_{ik}^2(t)/2\epsilon^2] \Big/ \sum_{i=1}^{n} \sum_{k=1}^{m} \exp[-u_{ik}^2(t)/2\epsilon^2].$$

It can be seen that using Eqs. (11) and (12) gives rise to monotonic increase of $P(t)$. Then by Proposition 3, the decrease of $P(t)$ will result in the increase of the minimal utility, in direct proportion to the value of λ_3.

Proposition 5. *Updating c_{ik} and r_{ik} by Eqs. (11) and (12) gives rise to monotonic increase of the whole utility of all the sensors, in direct proportion to the value of λ_2.*

Similar to Proposition 2, it follows that when a particle s_{ik} modifies its c_{ik} and r_{ik} by Eqs. (11) and (12), differentiation of $J(t)$ with respect to time t will not be negative—i.e., $\left\langle \frac{dJ_R(t)}{dt} \right\rangle \geqslant 0$, and it is directly proportional to the value of λ_2.

Proposition 6. *Updating c_{ik} and r_{ik} by Eqs. (11) and (12) gives rise to monotonic decrease of the potential energy $Q(t)$, in direct proportion to the value of λ_4.*

As in the above, we have

$$\left\langle \frac{du_{ik}(t)}{dt} \right\rangle_4 = -\lambda_4 \frac{\partial Q(t)}{\partial u_{ik}(t)} \left\{ \left[\frac{\partial u_{ik}(t)}{\partial r_{ik}(t)}\right]^2 + \left[\frac{\partial u_{ik}(t)}{\partial c_{ik}(t)}\right]^2 \right\}; \text{ and}$$

$$\begin{aligned}\left\langle \frac{dQ(t)}{dt} \right\rangle &= \frac{\partial Q(t)}{\partial u_{ik}(t)} \left\langle \frac{du_{ik}(t)}{dt} \right\rangle_4 = -\lambda_4 \left[\frac{\partial Q(t)}{\partial u_{ik}(t)}\right]^2 \\ &\quad \times \left\{ \left[\frac{\partial u_{ik}(t)}{\partial r_{ik}(t)}\right]^2 + \left[\frac{\partial u_{ik}(t)}{\partial c_{ik}(t)}\right]^2 \right\} \leqslant 0.\end{aligned}$$

Proposition 7. *C-GPM can dynamically optimize in parallel sensor resource allocation for a collection of sensors exhibiting different autonomous strengths of pursuing personal utility and executing social coordinations.*

In summary, by Propositions 1–6, $(\lambda_1 + \lambda_2)$ represents the autonomous strength for A_i to pursue its own personal utility; λ_2 represents the autonomous strength for A_i to take into account the collective utility of all the sensors; λ_3 represents the autonomous strength for A_i to increase the minimal personal utility among all the sensors; and λ_4 represents the autonomous strength for constraint satisfaction and social coordinations.

Propositions 1, 2, 3, 4 7 show that different sensors may have different degrees of autonomy and their own rationality in pursuing individual and system-wide benefits. Moreover, different sensors may engage in different social coordinations with other sensors for a specific object. A large variety of social coordinations may be taken into account, including possibly unilateral and unaware social coordinations.

3.3. Convergence analysis

In this subsection, we show that all the particles can converge to their stable equilibrium states through algorithm C-GPM.

Lemma 1. *If $\gamma - 1 > -\Psi_2(t) > 0$, $\frac{\partial \Psi_2(t)}{\partial u_{ik}(t)} < 1$ for $u_{ik}(t) > 1$, and $\frac{\partial \Psi_2(t)}{\partial u_{ik}(t)} > 1 - \gamma$ for $0 < u_{ik}(t) < 1$, then the particle s_{ik} will converge to a stable equilibrium point with $u_{ik}(t) > 1$, $v_{ik}(t) = 1$.*

Proof. For $\gamma > 1$, $\Psi_1(t)$ of particle s_{ik} is a piecewise linear function of the stimulus $u_{ik}(t)$, as shown in Fig. 4: Segment I, Segment II, and Segment III. By Eq. (9), a point is an equilibrium point, i.e., $du_{ik}(t)/dt = 0$, iff $-\Psi_2(t) = \Psi_1(t)$ at the point. We see that for the case of $\gamma - 1 > -\Psi_2(t) > 0$, an equilibrium point may be on Segment I, II or III. Note from Eq. (3), $u_{ik}(t) \geqslant 0$. Thus we need not consider the equilibrium point on Segment I.

Suppose that the particle s_{ik} is at an equilibrium point on Segment III at time t_0, and an arbitrarily small perturbation Δu_{ik} to the equilibrium point occurs at time t_1. Since $\frac{\partial \Psi_2(t)}{\partial u_{ik}(t)} < 1$, and $\frac{\partial \Psi_1(t)}{\partial u_{ik}(t)} = -1$ for $u_{ik}(t) > 1$, we have $c = \left[\frac{\partial \Psi_1(t)}{\partial u_{ik}(t)} + \frac{\partial \Psi_2(t)}{\partial u_{ik}(t)}\right] < 0$, and

$$\begin{aligned}\Delta \frac{du_{ik}}{dt} &= \left.\frac{du_{ik}}{dt}\right|_{t_1} - \left.\frac{du_{ik}}{dt}\right|_{t_0} = \left.\frac{du_{ik}}{dt}\right|_{t_1} = \Delta[\Psi_1(t) + \Psi_2(t)] \\ &\approx \left[\frac{\partial \Psi_1(t)}{\partial u_{ik}(t)} + \frac{\partial \Psi_2(t)}{\partial u_{ik}(t)}\right] \Delta u_{ik} = -|c| \Delta u_{ik}.\end{aligned}$$

That means $\left.\frac{du_{ik}}{dt}\right|_{t_1}$ is always against Δu_{ik}, or in other words, the perturbation will be suppressed and hence the particle s_{ik} will return to the original equilibrium point.

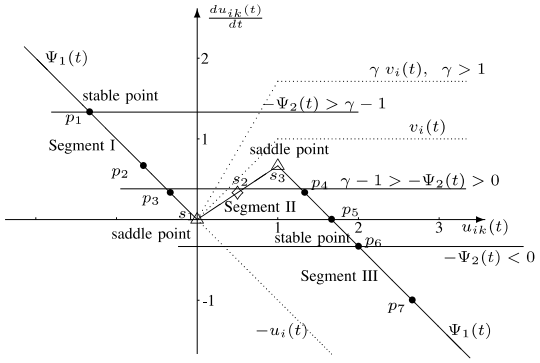

Fig. 4. When $\gamma > 1$, the reachable equilibrium points of the dynamic status $v_{ik}(t)$ of a particle s_{ik}. The point where $-\Psi_2(t)$ equals $\Psi_1(t)$ is an equilibrium point. ●, △ and ◊ denote a stable equilibrium point, saddle point and unstable equilibrium point, respectively.

Whereas, for an equilibrium point on Segment II, because $\frac{\partial \Psi_2(t)}{\partial u_{ik}(t)} > 1-\gamma$ and $\frac{\partial \Psi_1(t)}{\partial u_{ik}(t)} = \gamma - 1 > 0$, we have

$$c = \left[\frac{\partial \Psi_2(t)}{\partial u_{ik}(t)} + \frac{\partial \Psi_1(t)}{\partial u_{ik}(t)}\right] > 0, \quad \text{and} \quad \left.\frac{\mathrm{d}u_{ik}}{\mathrm{d}t}\right|_{t_1}$$
$$\approx \left[\frac{\partial \Psi_1(t)}{\partial u_{ik}(t)} + \frac{\partial \Psi_2(t)}{\partial u_{ik}(t)}\right]\Delta u_{ik} = |c|\Delta u_{ik}$$

such that the perturbation is intensified and the particle s_{ik} departs from the original equilibrium point on Segment II. Therefore, an equilibrium point on Segment II is unstable, and only an equilibrium point on Segment III, e.g., p_4 in Fig. 4, is stable with $u_{ik}(t) > 1, v_{ik}(t) = 1$. □

Lemma 2. *If* $\gamma > 1$, $-\Psi_2(t) < 0$, *and* $\frac{\partial \Psi_2(t)}{\partial u_{ik}(t)} < 1$ *for* $u_{ik}(t) > 1$, *then the particle* s_{ik} *will converge to a stable equilibrium point with* $u_{ik}(t) > 1$, $v_{ik}(t) = 1$.

Proof. Due to $\gamma > 1$ and $-\Psi_2(t) < 0$, an equilibrium point must be on Segment III, e.g., p_6 in Fig. 4. Moreover, as stated in the proof of Lemma 1, $\frac{\partial \Psi_2(t)}{\partial u_{ik}(t)} < 1$ for $u_{ik}(t) > 1$ guarantees any equilibrium point on Segment III to be stable, with $u_{ik}(t) > 1$, $v_{ik}(t) = 1$. □

Lemma 3. *If* $\gamma > 1$, $\frac{\partial \Psi_2(t)}{\partial u_{ik}(t)} < 1$ *for* $u_{ik}(t) = 1^+$; *and* $\frac{\partial \Psi_2(t)}{\partial u_{ik}(t)} > 1-\gamma$ *for* $u_{ik}(t) = 0^+$ *and* $u_{ik}(t) = 1^-$, *then the equilibrium points* s_1 *and* s_3 *in Fig. 4 are unstable and a saddle point, respectively.*

Proof. It is straightforward from the proof of Lemma 1. □

Theorem 1. *If* $\gamma > 1$, $\frac{\partial \Psi_2(t)}{\partial u_{ik}(t)} < 1$ *for* $u_{ik}(t) \geqslant 1^+$, *and* $\frac{\partial \Psi_2(t)}{\partial u_{ik}(t)} > 1-\gamma$ *for* $0^+ \leqslant u_{ik}(t) \leqslant 1^-$, *the dynamical equation (9) has a stable equilibrium point on Segment III iff the right side of the equation is larger than 0 for* $u_{ik}(t) = 1$ *and* $v_{ik}(t) = 1$.

Proof. By Lemmas 1–3, the equilibrium points on Segment II and Segment III, except for the saddle point s_3 in Fig. 4, are unstable and stable, respectively. We denote the right side of Eq. (9) by RHS.

Sufficiency. Assume that $\mathrm{RHS} = \frac{\mathrm{d}u_{ij}(t)}{\mathrm{d}t} = \Psi_1(t) + \Psi_2(t) > 0$ holds for $u_{ik}(t) = 1, v_{ik}(t) = 1$. It follows that $\Psi_1(t) \neq -\Psi_2(t)$ for $u_{ik}(t) = 1, v_{ik}(t) = 1$, namely, it is impossible that the equilibrium point is the intersection point s_3 where $\Psi_1(t) = -\Psi_2(t)$. Since $\mathrm{RHS} = \frac{\mathrm{d}u_{ik}}{\mathrm{d}t} > 0$ at point $u_{ik}(t) = 1$, $v_{ik}(t) = 1$, the increase of $u_{ik}(t)$ from value 1 leads to that the particle s_{ik} converges to a stable equilibrium point on Segment III.

Necessity. Suppose that Eq. (9) has a stable equilibrium point. We need to prove that $\mathrm{RHS} > 0$ holds for $u_{ik}(t) = 1$ and $v_{ik}(t) = 1$. By contrary, if there is $\mathrm{RHS} \leqslant 0$ for $u_{ik}(t) = 1$ and $v_{ik}(t) = 1$, then the equilibrium point must be either at the point s_3 where $\mathrm{RHS} = 0$, or on Segment II because $\mathrm{RHS} = \frac{\mathrm{d}u_{ik}}{\mathrm{d}t} < 0$ would give rise to the decrease of $u_{ik}(t)$ from value 1. Since the point s_3 and any equilibrium point on Segment II are all non-stable, we have a contradiction. □

Theorem 2. *If* $\gamma > 1$, $\frac{\partial \Psi_2(t)}{\partial u_{ik}(t)} < 1$ *for* $u_{ik}(t) \geqslant 1^+$, *and* $\frac{\partial \Psi_2(t)}{\partial u_{ik}(t)} > 1-\gamma$ *for* $0^+ \leqslant u_{ik}(t) \leqslant 1^-$, *then the dynamical equation (8) has a stable equilibrium point iff*

$$\gamma > 1 + 2[\lambda_3 + 0.25\lambda_4]. \tag{15}$$

Proof. By Eqs. (3), (4), (7), (8) we have

$$\begin{aligned}\Psi_2(t) = \{&\lambda_1 + \lambda_2 - \lambda_3\omega_{ik}^2(t)u_{ik}^2(t) \\ &- \lambda_4[(1+\exp(-\zeta_{ik}(t)u_{ik}(t)))^{-1} - 0.5]^2\}[r_{ik}^2(t) \\ &+ c_{ik}^2(t)][u_{ik}(t)]^2\end{aligned} \tag{16}$$

Note that $\omega_i^2(t), r_{ik}^2(t), c_{ik}^2(t) \leqslant 1$. By Theorem 1, for $u_{ik}(t) = 1$, $v_{ik}(t) = 1$, we have

$$\begin{aligned}\gamma &> 1 - \Psi_2(t) \\ &= 1 + \{-\lambda_1 - \lambda_2 + \lambda_3\omega_{ik}^2(t)u_{ik}^2(t) \\ &\quad + \lambda_4[(1+\exp(-\zeta_{ik}(t)u_{ik}(t)))^{-1} - 0.5]^2\}[r_{ik}^2(t) + c_{ik}^2(t)][u_{ik}(t)]^2 \\ &\leqslant 1 + 2[\lambda_3 + 0.25\lambda_4]. \qquad \square\end{aligned}$$

Lemma 4. *If* $\gamma > 1, \zeta_{ik}(t) \geqslant 0$, *and the following conditions are valid*:

$$\lambda_1 + \lambda_2 < (1 + 1/32)\lambda_3 + 0.25\lambda_4. \tag{17}$$

$$\gamma > \max\{1 + 4[\lambda_1 + \lambda_2 + 0.25\lambda_3 + \zeta_{ik}(t)\lambda_4], 1 + 2[\lambda_3 + 0.25\lambda_4]\}. \tag{18}$$

then the dynamical equation (9) has a stable equilibrium point with $u_{ik} = 1$, $v_{ik} = 1$.

Proof. Using Eq. (16) and noting $\frac{\mathrm{d}\omega_{ik}(t)}{\mathrm{d}u_{ik}(t)} = 2\omega_{ik}(t)u_{ik}(t)(\omega_{ik}(t) - 1)$, we obtain

$$\begin{aligned}\frac{\partial \Psi_2(t)}{\partial u_{ik}(t)} = \{&2[-\lambda_1 - \lambda_2 + \lambda_3\omega_{ik}^2(t)u_{ik}^2(t) \\ &+ \lambda_4[(1+\exp(-\zeta_{ik}(t)u_{ik}(t)))^{-1} - 0.5]^2] \\ &+ \left[-2\lambda_3\omega_{ik}(t)\frac{\mathrm{d}\omega_{ik}(t)}{\mathrm{d}u_{ik}(t)}u_{ik}^2(t) - 2\lambda_3\omega_{ik}^2(t)u_{ik}(t)\right. \\ &- 2\lambda_4\zeta_{ik}(t)\exp(-\zeta_{ik}(t)u_{ik}(t)) \\ &\times [(1+\exp(-\zeta_{ik}(t)u_{ik}(t)))^{-1} - 0.5] \\ &\left.\times [1+\exp(-\zeta_{ik}(t)u_{ik}(t))]^{-2}\right](-u_{ik}(t))\}x_{ik}^2(t)[r_{ik}^2(t) \\ &+ c_{ik}^2(t)][-u_{ik}(t)] = \{2[-\lambda_1 - \lambda_2 + \lambda_3\omega_{ik}^2(t)u_{ik}^2(t) \\ &+ \lambda_4[(1+\exp(-\zeta_{ik}(t)u_{ik}(t)))^{-1} - 0.5]^2] \\ &+ [-4\lambda_3\omega_{ik}^2(t)u_{ik}^3(t)(\omega_{ik}(t) - 1) - 2\lambda_3\omega_{ik}^2(t)u_{ik}(t) \\ &- 2\lambda_4\zeta_{ik}(t)\exp(-\zeta_{ik}(t)u_{ik}(t)) \\ &\times [(1+\exp(-\zeta_{ik}(t)u_{ik}(t)))^{-1} - 0.5] \\ &\times [1+\exp(-\zeta_{ik}(t)u_{ik}(t))]^{-2}](-u_{ik}(t))\}x_{ik}^2(t) \\ &\times [r_{ik}^2(t) + c_{ik}^2(t)][-u_{ik}(t)]\end{aligned}$$

Then from $\frac{\partial \Psi_2(t)}{\partial u_{ik}(t)} < 1$ for $u_{ik}(t) \geqslant 1^+$; and $u_{ik}(t) \leqslant \omega_{ik}(t)$, $r_{ik}(t), c_{ik}(t) \leqslant 1$, we derive

$$\frac{\partial \Psi_2(t)}{\partial u_{ik}(t)} < 2[2(-\lambda_1 - \lambda_2 + \lambda_3 + 0.25\lambda_4) + 4\lambda_3(2/3)^2(3/4)^3/12] < 1,$$

which leads to Eq. (17).

Similarly, from $\frac{\partial \Psi_2(t)}{\partial u_{ik}(t)} > 1 - \gamma$ for $0^+ \leqslant u_{ik}(t) \leqslant 1^-$, we have

$$\frac{\partial \Psi_2(t)}{\partial u_{ik}(t)} > 4(-\lambda_1 - \lambda_2 - \lambda_3/4 - \zeta_{ik}(t)\lambda_4) > 1 - \gamma,$$

which leads to Eq. (18). By Theorem 2, therefore the conclusion is valid. □

Lemma 5. *If $\gamma > 1, \zeta_{ik}(t) \leqslant 0$, and the following conditions are valid*:

$$\lambda_1 + \lambda_2 < (1 + 1/32)\lambda_3 + \lambda_4(|\zeta_{ik}(t)| + 0.25) \quad (19)$$

$$\gamma > \max\{1 + 4[\lambda_1 + \lambda_2 + 0.25\lambda_3], 1 + 2\lambda_3 + 0.25\lambda_4\} \quad (20)$$

then the dynamical equation (8) has a stable equilibrium point with $u_{ik} = 1,\ v_{ik} = 1$.

Proof. Similar to the proof of Lemma 4, from $\frac{\partial \Psi_2(t)}{\partial u_{ik}(t)} < 1$ for $u_{ik}(t) \geqslant 1^+$, and $u_{ik}(t) \leqslant; \omega_{ik}(t), r_{ik}(t), c_{ik}(t) \leqslant 1$, we derive

$$\frac{\partial \Psi_2(t)}{\partial u_{ik}(t)} < 2[2(-\lambda_1 - \lambda_2 + \lambda_3 + 0.25\lambda_4) + 4\lambda_3(2/3)^2(3/4)^3 1/12 + |\zeta_{ik}(t)|\lambda_4] < 1,$$

which leads to Eq. (19).

And from $\frac{\partial \Psi_2(t)}{\partial u_{ik}(t)} > 1 - \gamma$ for $0^+ \leqslant u_{ik}(t) \leqslant 1^-$, we have

$$\frac{\partial \Psi_2(t)}{\partial u_{ik}(t)} > 4(-\lambda_1 - \lambda_2 - \lambda_3/4) > 1 - \gamma,$$

which leads to Eq. (20). By Theorem 2, therefore the conclusion is valid. □

Theorem 3. *If $\gamma > 1$, and the conditions (18), (19) are valid, then the dynamical equation (9) has a stable equilibrium point with $u_{ik} = 1, v_{ik} = 1$.*

Proof. Straightforward, by Lemmas 4 and 5. □

Theorem 4. *If the conditions (17), (18) remain valid, then C-GPM will converge to a stable equilibrium state.*

Proof. Using Eq. (16) and noting $\frac{d\omega_{ik}(t)}{du_{ik}(t)} = 2\omega_{ik}(t)u_{ik}(t)(\omega_{ik}(t) - 1)$, we obtain

$$\begin{aligned}
\frac{\partial \Psi_2(t)}{\partial u_{ik}(t)} &= \{2[-\lambda_1 - \lambda_2 + \lambda_3\omega_{ik}^2(t)u_{ik}^2(t) \\
&\quad + \lambda_4[(1 + \exp(-\zeta_{ik}(t)u_{ik}(t)))^{-1} - 0.5]^2] \\
&\quad + [-2\lambda_3\omega_{ik}(t)\frac{d\omega_{ik}(t)}{du_{ik}(t)}u_{ik}^2(t) - 2\lambda_3\omega_{ik}^2(t)u_{ik}(t) \\
&\quad - 2\lambda_4\zeta_{ik}(t)\exp(-\zeta_{ik}(t)u_{ik}(t)) \\
&\quad \times [(1 + \exp(-\zeta_{ik}(t)u_{ik}(t)))^{-1} - 0.5] \\
&\quad \times \left[1 + \exp(-\zeta_{ik}(t)u_{ik}(t))\right]^{-2}](-u_{ik}(t))\}x_{ik}^2(t)[r_{ik}^2(t) \\
&\quad + c_{ik}^2(t)][-u_{ik}(t)] = \{2[-\lambda_1 - \lambda_2 + \lambda_3\omega_{ik}^2(t)u_{ik}^2(t) \\
&\quad + \lambda_4[(1 + \exp(-\zeta_{ik}(t)u_{ik}(t)))^{-1} - 0.5]^2] \\
&\quad + [-4\lambda_3\omega_{ik}^2(t)u_{ik}^3(t)(\omega_{ik}(t) - 1) - 2\lambda_3\omega_{ik}^2(t)u_{ik}(t) \\
&\quad - 2\lambda_4\zeta_{ik}(t)\exp(-\zeta_{ik}(t)u_{ik}(t)) \\
&\quad \times [(1 + \exp(-\zeta_{ik}(t)u_{ik}(t)))^{-1} - 0.5] \\
&\quad \times [1 + \exp(-\zeta_{ik}(t)u_{ik}(t))]^{-2}](-u_{ik}(t))\}x_{ik}^2(t)[r_{ik}^2(t) \\
&\quad + c_{ik}^2(t)][-u_{ik}(t)]
\end{aligned}$$

For the force field F, we define a Lyapunov function $L(t)$ by

$$\begin{aligned}
L(t) &= -\frac{1}{2}\sum_{i,k}(\gamma - 1)v_{ik}(t)^2 + \sum_{i,k}\int_0^t \frac{dv_{ik}(x)}{dx}\{-\lambda_1 - \lambda_2 \\
&\quad + \lambda_3\omega_{ik}^2(x)u_{ik}^2(x) + \lambda_4[(1 + \exp(-\zeta_{ik}(x)u_{ik}(x)))^{-1} \\
&\quad - 0.5]^2\}[r_{ik}^2(x) + c_{ik}^2(x)][-u_{ik}(x)]^2\,dx.
\end{aligned}$$

We hence have

$$\begin{aligned}
|L(t)| &\leqslant \sum_{i,k}(\gamma - 1)|v_{ik}(t)^2| + \sum_{i,k}\int_0^t \left|\frac{dv_{ik}(x)}{dx}\right| \cdot |\{-\lambda_1 - \lambda_2 \\
&\quad + \lambda_3\omega_{ik}^2(x)u_{ik}^2(x) + \lambda_4[(1 + \exp(-\zeta_{ik}(x)u_{ik}(x)))^{-1} \\
&\quad - 0.5]^2\}|[r_{ik}^2(x) + c_{ik}^2(x)][-u_{ik}(x)]^2\,dx.
\end{aligned}$$

Since condition (18) is valid, $v_{ik}(t) \leqslant 1$ and $u_i(t) \leqslant 1$, it follows that

$$|L(t)| \leqslant \sum_{i,k}(\gamma - 1) + \sum_{i,k}\gamma < mn\gamma$$

which implies that $L(t)$ is bounded.

In addition, we have

$$\begin{aligned}
\frac{dL(t)}{dt} &= -\sum_{i,k}(\gamma - 1)v_{ik}(t)\frac{dv_{ik}(t)}{dt} + \sum_{i,k}\frac{dv_{ik}(t)}{dt}\{-\lambda_1 - \lambda_2 \\
&\quad + \lambda_3\omega_{ik}^2(t)u_{ik}^2(t) + \lambda_4[(1 + \exp(-\zeta_{ik}(t)u_{ik}(t)))^{-1} \\
&\quad - 0.5]^2\}[r_{ik}^2(t) + c_{ik}^2(t)][-u_{ik}(t)]^2 \\
&= -\sum_{i,k}\frac{dv_{ik}(t)}{du_i(t)}\frac{du_{ik}(t)}{dt}\{-u_{ik}(t) + \gamma v_{ik}(t) + \{\lambda_1 + \lambda_2 \\
&\quad - \lambda_3\omega_{ik}^2(t)u_{ik}^2(t) - \lambda_4[(1 + \exp(-\zeta_{ik}(t)u_{ik}(t)))^{-1} \\
&\quad - 0.5]^2\}[r_{ik}^2(t) + c_{ik}^2(t)][-u_{ik}(t)]^2\} \\
&= -\sum_{i,k}\frac{dv_{ik}(t)}{du_{ik}(t)}\left(\frac{du_{ik}(t)}{dt}\right)^2 \leqslant 0.
\end{aligned}$$

Thus $L(t)$ will monotonically decrease with the elapsing time. □

3.4. The parallel C-GPM algorithm

Algorithm C-GPM

Input: $c_{ik}, x_{ik}, \zeta_{ik}$
Output:
1. Initialization:
   $t \leftarrow 0$
   $r_{ik}(t)$ —Initialize in parallel
2. **While** $(\mathrm{d}u_{ik}/\mathrm{d}t \neq 0)$ **do**
$t \leftarrow t+1$
$u_{ik}(t)$ —Compute in parallel according to Eq. (3)
$\mathrm{d}u_{ik}/\mathrm{d}t$ —Compute in parallel according to Eq. (8)
$\mathrm{d}r_{ik}(t)/\mathrm{d}t$ —Compute in parallel according to Eq. (11)
$r_{ik}(t) \leftarrow r_{ik}(t-1) + \mathrm{d}r_{ik}(t)/\mathrm{d}t$
$\mathrm{d}c_{ik}(t)/\mathrm{d}t$ —Compute in parallel according to Eq. (10)
$c_{ik}(t) \leftarrow c_{ik}(t-1) + \mathrm{d}c_{ik}(t)/\mathrm{d}t$

As indicated by Theorems 1–4, as long as we properly select the parameters $\lambda_1, \lambda_2, \lambda_3, \lambda_4$ for the dynamical equations of C-GPM according to Eqs. (17), (19), the convergence and stability of the particle dynamics can be guaranteed.

Given the results above, we can construct an algorithm to solve the sensor fusion (resource allocation) problem, as given below.

The algorithm C-GPM has in general a complexity of $\Omega(nm)$, where (nm) is the number of particles (the sum of the number of elements of matrix $\mathscr{S}$). The more realistic time complexity of the algorithm is $O(I)$, where I is the number of iterations for Step 2 (the while loop), as much of the inner steps can be carried out in parallel.

4. Simulations

Here we give an example of a robot which represents a multi-sensor fusion problem, and then use our C-GPM method to find the optimum solution.

The robot has seven sensors: eye, nose, ear, arm, hand, leg and foot. The robot has a reportoire of three actions: open a door, take dictation, find food and take back. Now we describe in detail how to solve the multi-sensor fusion problem, namely, how to allocate sensors to objects.

Let sensors $A_i,\ i = 1, 2, \ldots, 7$ represent the eye, nose, ear, arm, hand, leg and foot of the robot, respectively. Let objects $T_k,\ k = 1, 2, 3$ represent the robot's actions of opening a door, taking dictation, and finding food and taking them back, respectively.

Step 1.

1. x_{ik}:

First, we establish the relations between sensors and objects (actions). If sensor A_i is related to object T_k, $x_{ik} = 1$; otherwise, $x_{ik} = 0$. For example, the eye, arm, hand, leg and foot are related to the object of opening a door; the eye, ear, arm and hand are related to the object of taking dictation. We can form the matrix X, as follows:

x_{ik}	T_1 open a door	T_2 take dictation	T_3 find food and take back
A_1: eye	1	1	1
A_2: nose	0	0	1
A_3: ear	0	1	0
A_4: arm	1	1	1
A_5: hand	1	1	1
A_6: leg	1	0	1
A_7: foot	1	0	1

2. c_{ik}:

Based on the different effects of the sensors A_1–A_7 on the objects T_1–T_3, we can choose different weights c_{ik}. If sensor A_i is more important to object T_k than to T_l $(k, l \in 1, 2, 3)$, then c_{ik} will be larger than c_{il}. The following must be observed when choosing the weights:

- If $x_{ik} = 0$, then $c_{ik} = 0$, to ensure that object T_k which is not related to sensor A_i is not allocated any sensor resource.
- $0 \leqslant c_{ik} \leqslant 1$.
- In order that the sensor resources are fully allocated, $\sum_{k=1}^{3} c_{ik} = 1,\ i = 1, 2, \ldots, 7$.

The weight matrix C we decide on for this particular problem is as follows:

c_{ik}	T_1 open a door	T_2 take dictation	T_3 find food and take back
A_1: eye	0.5	0.25	0.25
A_2: nose	0	0	1
A_3: ear	0	1	0
A_4: arm	0.4	0.3	0.4
A_5: hand	0.33	0.34	0.33
A_6: leg	0.35	0	0.65
A_7: foot	0.35	0	0.65

3. ζ_{ik}:

(1) β_{ijk}:

C-GPM has a clear advantage over other approaches in being able to deal with a variety of coordinations occurring in multi-sensor systems. In Section 3, we divide typical coordinations into four categories (I, II, III, IV) of 12 types.

Since the nose A_2 is not related with the object T_1 of opening a door, the coordination of the eye A_1 with respect to the nose A_2 is unilateral coordination, whereby A_2 would modify its intention, and A_1 would not. Therefore, $\beta_{121} = \mathrm{II}$ and $\beta_{211} = \mathrm{I}$. Since the eye A_1 and the arm A_4

are both related to the object T_1 of opening a door, but they themselves are unrelated, the coordination between the eye A_1 and the arm A_4 is bilateral coordination, and neither A_1 nor A_4 would modify their intention. So $\beta_{141} = \text{III}$ and $\beta_{411} = \text{III}$. Since the arm A_4 and the hand A_5 are both related to the object T_1 of opening a door and they influence each other, the coordination between A_4 and A_5 is bilateral coordination, and A_4 and A_5 must both modify their intention. So $\beta_{451} = \text{IV}$ and $\beta_{541} = \text{IV}$.

As such, we can obtain all the β_{ijk} values, as shown in the following, where for object T_k, if there is no coordination between sensor A_i and A_j, β_{ijk} is set to "–".

β_{ij1}	A_1	A_2	A_3	A_4	A_5	A_6	A_7
A_1	–	II	II	III	III	III	III
A_2	I	–	–	I	I	I	I
A_3	I	–	–	I	I	I	I
A_4	III	II	II	–	IV	III	III
A_5	III	II	II	IV	–	III	III
A_6	III	II	II	III	III	–	IV
A_7	III	II	II	III	III	IV	–

β_{ij2}	A_1	A_2	A_3	A_4	A_5	A_6	A_7
A_1	–	II	III	III	III	II	II
A_2	I	–	I	I	I	–	–
A_3	III	II	–	III	III	II	II
A_4	III	II	III	–	IV	II	II
A_5	III	II	III	IV	–	II	II
A_6	I	–	I	I	I	–	–
A_7	I	–	I	I	I	–	–

β_{ij3}	A_1	A_2	A_3	A_4	A_5	A_6	A_7
A_1	–	III	II	III	III	III	III
A_2	III	–	II	III	III	III	III
A_3	I	I	–	I	I	I	I
A_4	III	III	II	–	IV	III	III
A_5	III	III	II	IV	–	III	III
A_6	III	III	II	III	III	–	IV
A_7	III	III	II	III	III	IV	–

(2) ζ_{ijk}:

According to Eq. (6),

$$\zeta_{ijk}(t) = \begin{cases} 1 & \text{if } \beta_{ijk} \in \mathscr{L}^{(\text{II})} \cup \mathscr{L}^{(\text{III})} \\ -1 & \text{if } \beta_{ijk} \in \mathscr{L}^{(\text{I})} \cup \mathscr{L}^{(\text{IV})} \end{cases}$$

$$\zeta_{jik}(t) = \begin{cases} 1 & \text{if } \beta_{jik} \in \mathscr{L}^{(\text{I})} \cup \mathscr{L}^{(\text{III})} \\ -1 & \text{if } \beta_{jik} \in \mathscr{L}^{(\text{II})} \cup \mathscr{L}^{(\text{IV})} \end{cases}$$

and so we obtain ζ_{ijk} as follows:

ζ_{ij1}	A_1	A_2	A_3	A_4	A_5	A_6	A_7
A_1	0	1	1	1	1	1	1
A_2	−1	0	0	−1	−1	−1	−1
A_3	−1	0	0	−1	−1	−1	−1
A_4	1	1	1	0	−1	1	1
A_5	1	1	1	−1	0	1	1
A_6	1	1	1	1	1	0	−1
A_7	1	1	1	1	1	−1	0

ζ_{ij2}	A_1	A_2	A_3	A_4	A_5	A_6	A_7
A_1	0	1	1	1	1	1	1
A_2	−1	0	−1	−1	−1	0	0
A_3	1	1	0	1	1	1	1
A_4	1	1	1	0	−1	1	1
A_5	1	1	1	−1	0	1	1
A_6	−1	0	−1	−1	−1	0	0
A_7	−1	0	−1	−1	−1	0	0

ζ_{ij3}	A_1	A_2	A_3	A_4	A_5	A_6	A_7
A_1	0	1	1	1	1	1	1
A_2	1	0	1	1	1	1	1
A_3	−1	−1	0	−1	−1	−1	−1
A_4	1	1	1	0	−1	1	1
A_5	1	1	1	−1	0	1	1
A_6	1	1	1	1	1	0	−1
A_7	1	1	1	1	1	−1	0

(3) ζ_{ik}:

According to Eq. (5), $\zeta_{ik}(t) = \sum_{j=1}^{n} \zeta_{ijk}(t) + \sum_{j=1}^{n} \zeta_{jik}(t)$, we get ζ_{ik} as follows:

ζ_{ik}	T_1	T_2	T_3
A_1	8	6	10
A_2	0	0	10
A_3	0	6	0
A_4	4	2	6
A_5	4	2	6
A_6	4	0	6
A_7	4	0	6

ζ_{ik} is equal to the sum of the ith row and the ith column of the matrix $(\zeta_{ijk})_{7\times 7}$.

4. r_{ik}:

Initialization: $(t = 0)$

r_{ik}	T_1	T_2	T_3
A_1	1/3	1/3	1/3
A_2	0	0	1
A_3	0	1	0
A_4	1/3	1/3	1/3
A_5	1/3	1/3	1/3
A_6	1/2	0	1/2
A_7	1/2	0	1/2

Here r_{ik} is initialized by the average values. Alternatively, r_{ik} can also be initialized as random numbers between 0 and 1. In fact, based on the experiments we have done, we found that the results are not affected by the initialization of R. Whatever r_{ik} is initialized to be, the matrix R is dealt with using the following three steps:

- $r_{ik} = 0 | \forall x_{ik} = 0$. If $x_{ik} = 0$, then $r_{ik} = 0$, to ensure that an object T_k which is not related to the sensor A_i is not allocated any sensor resource.
- Non-negativity: $0 \leqslant r_{ik} \leqslant 1$. If $\min_{i,k} r_{ik} < 0$, then let $r_{ik} = r_{ik} - \min_{i,k} r_{ik}$.
- Normalization. Let $r_{ik} = r_{ik} / \sum_{k=1}^{3} r_{ik}$, in order that the sensor resources are fully allocated; that is, $\sum_{k=1}^{3} r_{ik} = 1,\ i = 1, 2, \ldots, 7$.

5. $z(R)$:

According to Eq. (1), $z(R) = \sum_{i=1}^{n} \sum_{k=1}^{m} c_{ik} r_{ik} x_{ik} = 4.023$.

Step 2. Compute in parallel (showing only the first evolutionary iteration; $t = 1$).

1. Δr_{ik}:

According to Eq. (11), we have

$$\Delta r_{ik} \approx \mathrm{d}r_{ik}/\mathrm{d}t = \lambda_1 \frac{\partial u_{ik}}{\partial r_{ik}} + \lambda_2 \frac{\partial J}{\partial r_{ik}} - \lambda_3 \frac{\partial P}{\partial r_{ik}} - \lambda_4 \frac{\partial Q}{\partial r_{ik}}$$

where,

$$\frac{\partial u_{ik}}{\partial r_{ik}} = c_{ik} x_{ik} \exp(-c_{ik} r_{ik} x_{ik})$$

$$\frac{\partial J}{\partial r_{ik}} = c_{ik} x_{ik} \exp(-c_{ik} r_{ik} x_{ik})$$

$$\frac{\partial P}{\partial r_{ik}} = \frac{\partial P}{\partial u_{ik}} \cdot \frac{\partial u_{ik}}{\partial r_{ik}} = -u_{ik} \cdot \frac{\exp(-u_{ik}^2/2\epsilon^2)}{\sum_{i=1}^{n}\sum_{k=1}^{m} \exp(-u_{ik}^2/2\epsilon^2)} \cdot \frac{\partial u_{ik}}{\partial r_{ik}}$$

$$\frac{\partial Q}{\partial r_{ik}} = 2 \sum_{k=1}^{m} x_{ik} \cdot \sum_{i=1}^{n} \left(\sum_{k=1}^{m} r_{ik} x_{ik} - 1 \right) - \left[\frac{1}{1 + \exp(-\zeta_{ik} u_{ik})} - \frac{1}{2} \right] \cdot \frac{\partial u_{ik}}{\partial r_{ik}}$$

2. Δc_{ik}:

According to Eq. (10), we have

$$\Delta c_{ik} \approx \mathrm{d}c_{ik}/\mathrm{d}t = \lambda_1 \frac{\partial u_{ik}}{\partial c_{ik}} + \lambda_2 \frac{\partial J}{\partial c_{ik}} - \lambda_3 \frac{\partial P}{\partial c_{ik}} - \lambda_4 \frac{\partial Q}{\partial c_{ik}}$$

where,

$$\frac{\partial u_{ik}}{\partial c_{ik}} = r_{ik} x_{ik} \exp(-c_{ik} r_{ik} x_{ik})$$

$$\frac{\partial J}{\partial c_{ik}} = r_{ik} x_{ik} \exp(-c_{ik} r_{ik} x_{ik})$$

$$\frac{\partial P}{\partial c_{ik}} = \frac{\partial P}{\partial u_{ik}} \cdot \frac{\partial u_{ik}}{\partial c_{ik}} = -u_{ik} \cdot \frac{\exp(-u_{ik}^2/2\epsilon^2)}{\sum_{i=1}^{n}\sum_{k=1}^{m} \exp(-u_{ik}^2/2\epsilon^2)} \cdot \frac{\partial u_{ik}}{\partial c_{ik}}$$

$$\frac{\partial Q}{\partial c_{ik}} = -\left[\frac{1}{1 + \exp(-\zeta_{ik} u_{ik})} - \frac{1}{2} \right] \cdot \frac{\partial u_{ik}}{\partial c_{ik}}$$

3. $r_{ik}(t = 1)$ and $c_{ik}(t = 1)$:

$$r_{ik}(t = 1) = r_{ik}(t = 0) + \Delta r_{ik}(t = 1)$$

$$c_{ik}(t = 1) = c_{ik}(t = 0) + \Delta c_{ik}(t = 1)$$

$$\lambda_1 = 0.05 \quad \lambda_2 = 0.05 \quad \lambda_3 = 0.9 \quad \lambda_4 = 0.9 \quad \epsilon = 0.8$$

After we get $r_{ik}(t = 1)$, matrix R should be dealt with using the three steps just mentioned again.

In addition, after we get $c_{ik}(t = 1)$, matrix C should be dealt with similarly, i.e.,

- $c_{ik} = 0 | \forall x_{ik} = 0$.
- Non-negativity: Let $c_{ik} = c_{ik} - \min_{i,k} c_{ik}$.
- Normalization. Let $c_{ik} = c_{ik} / \sum_{k=1}^{3} c_{ik}$.

Regarding the coefficients λ_1, λ_2, λ_3, λ_4 and ϵ, we can draw the following conclusions from the theoretical proofs and the experiments we have done:

- When ϵ is larger, the convergence speed of C-GPM algorithm is faster.
- If the values of λ_1, λ_2, λ_3, and λ_4 change in direct proportion, the experimental results will hardly be influenced.
- In order for the C-GPM algorithm to converge, λ_3 and λ_4 should be much larger than λ_1 and λ_2, based on Eqs. (17) and (19).

At the end of the first iteration we get

$$R(t = 1) = \begin{pmatrix} 0.3692 & 0.3111 & 0.3197 \\ 0 & 0 & 1.0000 \\ 0 & 1.0000 & 0 \\ 0.3368 & 0.3158 & 0.3474 \\ 0.3331 & 0.3260 & 0.3409 \\ 0.4582 & 0 & 0.5418 \\ 0.4582 & 0 & 0.5418 \end{pmatrix}$$

$$C(t = 1) = \begin{pmatrix} 0.4869 & 0.2483 & 0.2648 \\ 0 & 0 & 1.0000 \\ 0 & 1.0000 & 0 \\ 0.3603 & 0.2661 & 0.3735 \\ 0.3304 & 0.3269 & 0.3427 \\ 0.3554 & 0 & 0.6446 \\ 0.3554 & 0 & 0.6446 \end{pmatrix}$$

$$z(t = 1) = 4.0690$$

Obviously, $z(t = 1) > z(t = 0)$, the robot multi-sensor fusion problem is being optimized. The evolutionary experimental results for z from $t = 1$ to $t = 120$ are as follows, and depicted in Fig. 5.

As shown in Fig. 5, the convergence speed is faster at the beginning (from $t = 0$ to $t = 20$) of the evolution. The

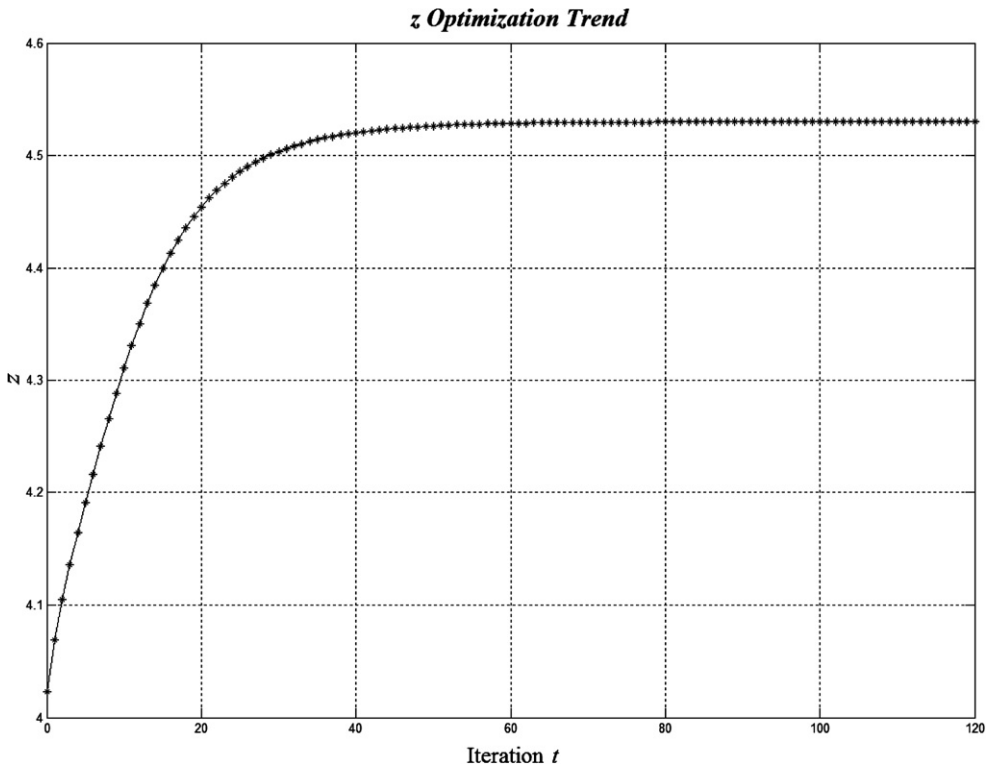

Fig. 5. Optimization from $t = 0$ to $t = 120$.

optimization trend of z reflects exactly the optimization of the problem. At about $t = 60$, z approaches the maximum of 4.53. At $t = 96$, z reaches its maximum, and stays unchanged in the remainder of the iterations. From $t = 104$ to 120, R is always equal to

$$\begin{pmatrix} 1.0000 & 0.0000 & 0.0000 \\ 0 & 0 & 1.0000 \\ 0 & 1.0000 & 0 \\ 0.0000 & 0.0000 & 1.0000 \\ 0.0000 & 0.0000 & 1.0000 \\ 0.0000 & 0 & 1.0000 \\ 0.0000 & 0 & 1.0000 \end{pmatrix}$$

Since $r_{ik}(t = 104) = r_{ik}(t = 105)$ and $c_{ik}(t = 104) = c_{ik}(t = 105)$, $\mathrm{d}r_{ik}/\mathrm{d}t(t = 105) = 0$ and $\mathrm{d}c_{ik}/\mathrm{d}t(t = 105) = 0$. Thus, $\frac{\mathrm{d}u_{ik}}{\mathrm{d}t}(t = 105) = \frac{\partial u_{ik}}{\partial r_{ik}}(t = 105)\frac{\mathrm{d}r_{ik}}{\mathrm{d}t}(t = 105) + \frac{\partial u_{ik}}{\partial c_{ik}}(t = 105)\frac{\mathrm{d}c_{ik}}{\mathrm{d}t}(t = 105) = 0$. Therefore, the C-GPM algorithm ends appropriately. This shows that sensor resources are allocated to the objects whose weights are the maximum. Undoubtedly this solution of R obtained by C-GPM is the optimum solution as it maximizes z, which verifies the approach's convergence and its ability to arrive at the optimum for a complex problem. The solution at $t = 120$ however is not a practical solution because in order to achieve the objective, it does not give the "less important" sensors any resource. A more practical solution is probably at around $t = 20$ where z is very near its maximum value and every sensor is allocated some resource:

$$\begin{pmatrix} 0.8852 & 0.0277 & 0.0871 \\ 0 & 0 & 1.0000 \\ 0 & 1.0000 & 0 \\ 0.1041 & 0.0426 & 0.8533 \\ 0.1037 & 0.0565 & 0.8398 \\ 0.0723 & 0 & 0.9277 \\ 0.0723 & 0 & 0.9277 \end{pmatrix}$$

It should be possible to re-formulate the problem model, perhaps with the addition of more constraints, such that the iterative algorithm will settle at an optimum yet practical solution.

Besides the C-GPM algorithm's good performance in the mathematical sense, the particles' evolution and motion during the process of resolving the problem are also very interesting. If $x_{ik} = 1$, then s_{ik} is a particle. For our robot problem, there are 15 particles.

s_{ik}	T_1	T_2	T_3
A_1	•	•	•
A_2			•
A_3		•	
A_4	•	•	•
A_5	•	•	•
A_6	•		•
A_7	•		•

According to Eq. (3), $u_{ik} = 1 - \exp(-c_{ik} r_{ik} x_{ik})$, we get $u_{ik}(t = 0)$, as follows:

$u_{ik}(t = 0)$	T_1	T_2	T_3
A_1	0.1521	0.0792	0.0792
A_2	0	0	0.6321
A_3	0	0.6321	0
A_4	0.1237	0.0943	0.1237
A_5	0.1032	0.1061	0.1032
A_6	0.1605	0	0.2775
A_7	0.1605	0	0.2775

u_{ik} is the y-coordinate of particle s_{ik}. The x-coordinate of particle s_{ik} represents the ordinal number of the particle.

The initial states of the 15 particles in the force field are shown in Fig. 6.

When $t = 5$, 10, 15, 120, the states of the 15 particles in the force field are shown in Figs. 7–10, respectively.

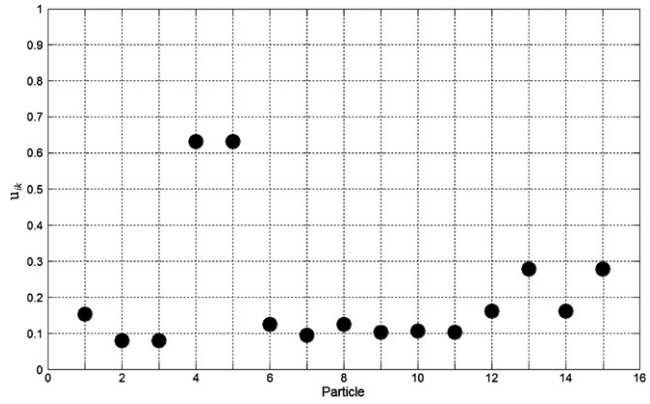

Fig. 6. The initial state of 15 particles in the force field.

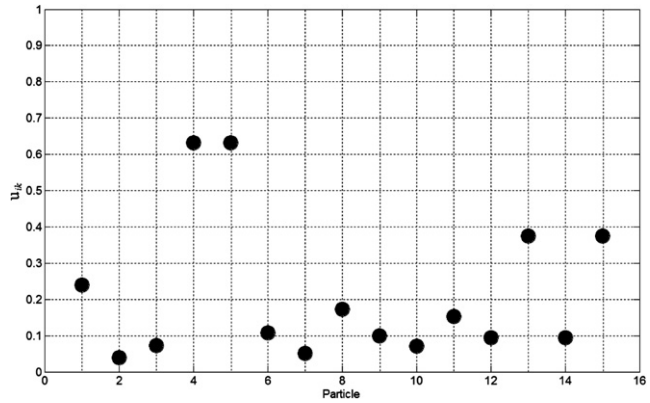

Fig. 7. When $t = 5$.

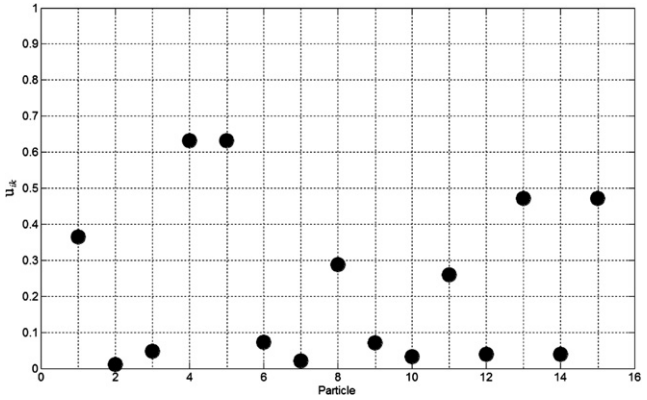

Fig. 8. When $t = 10$.

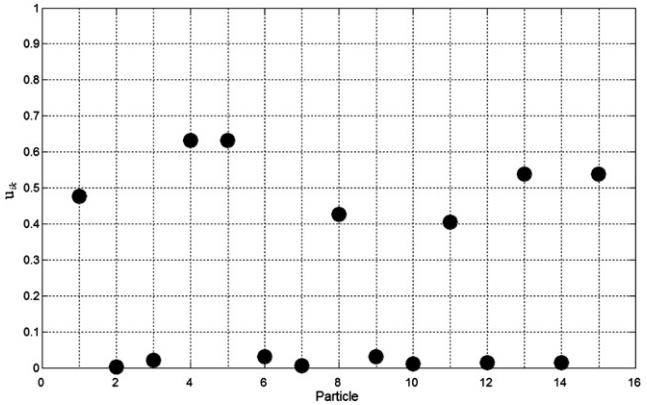

Fig. 9. When $t = 15$.

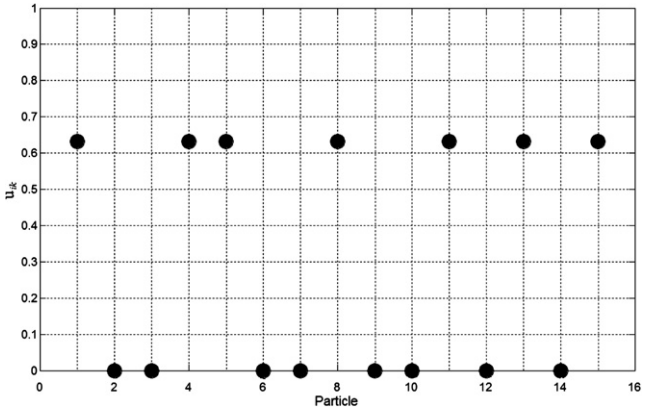

Fig. 10. When $t = 120$.

5. Conclusion

In this paper, we describe a new evolutionary approach to multi-sensor fusion based on the coordination generalized particle model (C-GPM). We study some theoretical foundations of the approach including its convergence. The validity of C-GPM is verified via several formal proofs and by simulations.

We present the C-GPM approach as a new branch of evolutionary algorithms, which can overcome the limitations of other existing evolutionary algorithms in capturing the entire dynamics inherent in the problem, especially those that are high-dimensional, highly nonlinear, and random.

Hence, the C-GPM approach can describe the complex behaviors and dynamics of multiple sensors.

The model treats each possible allocation of resources as a configuration of particles with "physical" attributes and then finds the equilibrium of the system iteratively. A novel aspect of the approach is that it takes into account "unconscious" social coordinations between the sensors.

The C-GPM algorithm can work out the theoretical optimum solution, which is important and exciting. To summarize, the C-GPM approach has the following attractive features:

- Very high parallelism and real-time computational performance.
- A sensor in a multi-sensor system is regarded as being neither fully selfish nor fully unselfish, and so different sensors can exhibit different degrees of autonomy.
- A variety of complicated social coordinations among the sensors can be taken into account in the process of problem-solving.
- The C-GPM algorithm can work out the optimum solution of any multi-sensor fusion problem.
- C-GPM is a physics-based evolutionary algorithm that can overcome the limitations of other traditional evolutionary algorithms in describing the high-dimensional, highly nonlinear, and random behaviors and dynamics of objects.
- There are only five coefficients in the C-GPM algorithm, whose values are all easy to choose.

Acknowledgements

We thank the editor and referees for their very clear and useful advice and comments. This work is supported by a Hong Kong University Small Project Funding (200607176155).

References

[1] S. Forrest, Genetic algorithms—principles of natural-selection applied to computation, Science 261 (5123) (1993) 872–878.
[2] S. Kirkpatrick, C.D. Gelatt, M.P. Vecchi, Optimization by simulated annealing, Science 220 (4598) (1983) 671–680.
[3] E. Bonabeau, M. Dorigo, G. Theraulaz, Inspiration for optimization from social insect behaviour, Nature 406 (6791) (2000) 39–42.
[4] J. Kennedy, R.C. Eberhart, Particle swarm optimization, in: Proc. IEEE Conf. Neural Networks, Piscataway, NJ, vol. IV, 1995, pp. 1942–1948.
[5] Z. Ren, C.J. Anumba, O.O. Ugwu, The development of a multi-agent system for construction claims negotiation, Advances in Engineering Software 34 (2003) 683–696.
[6] Z. Ren, C.J. Anumba, Multi-agent systems in construction state of the art and prospects, Automation in Construction 13 (2004) 421–434.
[7] G. Vincent, L.P. Christophe, S. Sami, A multi-agents architecture to enhance end-user individual based modelling, Ecological Modelling 157 (2002) 23–41.
[8] C.J. Emmanouilides, S. Kasderidis, J.G. Taylor, A random asymmetric temporal model of multi-agent interactions: dynamical analysis, Physica D 181 (2003) 102–120.